Delft University of Technology

Analyzing Cascading Failures in Power Grids under the AC and DC Power Flow Models

Cetinay-Iyicil, Hale; Soltan, Saleh; Kuipers, Fernando A.; Zussman, Gil; Van Mieghem, Piet

Important note
To cite this publication, please use the final published version (if applicable).
Please check the document version above.

Analyzing Cascading Failures in Power Grids under the AC and DC Power Flow Models

Hale Cetinay
Faculty of Electrical Engineering, Mathematics and Computer Science,
Delft University of Technology
Delft, Netherlands
H.Cetinay-Iyicil@tudelft.nl

Saleh Soltan
Electrical Engineering
Princeton University
Princeton, NJ, USA
ssoltan@princeton.edu

Fernando A. Kuipers
Faculty of Electrical Engineering, Mathematics and Computer Science,
Delft University of Technology
Delft, Netherlands
F.A.Kuipers@tudelft.nl

Gil Zussman
Electrical Engineering
Columbia University
New York, NY, USA
gil@ee.columbia.edu

Piet Van Mieghem
Faculty of Electrical Engineering, Mathematics and Computer Science,
Delft University of Technology
Delft, Netherlands
P.F.A.VanMieghem@tudelft.nl

ABSTRACT

In this paper, we study cascading failures in power grids under the nonlinear AC and linearized DC power flow models. We numerically compare the evolution of cascades after single line failures under the two flow models in four test networks. The cascade simulations demonstrate that the assumptions underlying the DC model (e.g., ignoring power losses, reactive power flows, and voltage magnitude variations) can lead to inaccurate and overly optimistic cascade predictions. Particularly, in large networks the DC model tends to overestimate the yield (the ratio of the demand supplied at the end of the cascade to the initial demand). Hence, using the DC model for cascade prediction may result in a misrepresentation of the gravity of a cascade.

Keywords

Power grids, AC versus DC, power flows, cascading failures, contingency analysis.

1. INTRODUCTION

Power grids are vulnerable to external events, such as natural disasters and cyber-attacks, as well as to internal events, such as unexpected variability in load or generation, aging, and control device malfunction. The operation of a power grid is governed by the laws of physics [13], and the outage of an element may result in a cascade of failures and a blackout [6]. The recent blackouts in Turkey [2], India [5], U.S. and Canada [3] had devastating effects and as such motivated the study of power grid vulnerabilities to cascading failures (e.g., [4, 6, 8, 16]).

Some of the recent work on cascading failures considers a topological perspective where, once a network element fails,

the neighboring elements also fail [10]. However, such topological models do not consider the actual power grid flow dynamics. More realistic cascading failures models use the linearized direct current (DC) power flows [14, 17]. However, DC power flows are based on a linearization of the nonlinear AC power flow dynamics. The induced linearization error can be small in large transmission grids [15] and high for some particular networks [18]. Motivated by these observations, *we study the cascading failures under both the linearized DC model and a nonlinear AC model* by performing simulations on four test networks.

We present an AC cascading failures model that is based on the nonlinear power flow equations, and therefore, is more realistic than the corresponding DC model. We empirically compare the AC and DC cascade models based on robustness metrics that quantify the operational and topological characteristics of the grid during a cascade for all cascading failures initiated by single line failures. Our simulations demonstrate that the assumptions underlying the DC model (lossless network assumption, and ignoring reactive power flows and voltage variations) can lead to inaccurate and overly optimistic cascade predictions. For example, in the Polish grid, the difference between the yield (the ratio of the demand supplied at the end of the cascade to the initial demand) under the AC and DC cascade models is more than 0.4, in 60% of the cascades initiated by single line failures.

Moreover, we empirically compare the AC and DC cascades under different supply and demand balancing and line outage rules. Our simulation results show that the difference between the cascade evolution under the AC and DC power flows depends on the balancing and line outage rules in power grids. In particular, the supply and demand balancing rule, which separates the excess supply or demand from the grid, increases the difference between the AC and DC models the most.

The remainder of this paper is organized as follows. Section 2 presents the power flow equations. Section 3 presents

the cascading failures models. Section 4 presents the numerical comparison of the AC and DC flow models in four different test networks and Section 5 concludes the paper.

2. POWER FLOW EQUATIONS

In this section, we provide details on the AC and DC power flow equations.

2.1 AC Power Flow Equations

A power grid with n nodes (buses) and m transmission lines constitutes a complex network whose underlying topology can be represented by an undirected graph $\mathcal{G}(\mathcal{N}, \mathcal{L})$, where $\mathcal{N}$ denotes the set of nodes and $\mathcal{L}$ denotes the set of lines. Each line l has a predetermined capacity c_l that bounds its flow $|f_l|$ under a normal operation of the system. The status of each node i is represented by its voltage $V_i = |V_i|e^{i\theta_i}$ in which $|V_i|$ is the voltage magnitude, θ_i is the phase angle at node i, and $\mathbf{i}$ denotes the imaginary unit. In the steady-state, the injected apparent power S_i at node i equals to

$$S_i = V_i(\mathbf{YV})_i^* \qquad (1)$$

where * denotes the complex conjugation, $\mathbf{V} = [V_1, \ldots, V_n]^{\mathrm{T}}$ is the vector of node voltages, and $\mathbf{Y}$ is the $n \times n$ admittance matrix [13].

Rewriting the admittance matrix as $\mathbf{Y} = \mathbf{G} + \mathbf{iB}$ where $\mathbf{G}$ and $\mathbf{B}$ are real matrices, and using the definition of the apparent power $S_i = P_i + \mathbf{i}Q_i$ in (1) leads to the equations for the active power P_i and the reactive power Q_i at each node i:

$$P_i = \sum_{k=1}^{n} |V_i||V_k|(G_{ik}\cos\theta_{ik} + B_{ik}\sin\theta_{ik}) \qquad (2)$$

$$Q_i = \sum_{k=1}^{n} |V_i||V_k|(G_{ik}\sin\theta_{ik} - B_{ik}\cos\theta_{ik}) \qquad (3)$$

where $\theta_{ik} = \theta_i - \theta_k$.

2.2 DC Power Flow Equations

The AC power flow equations are nonlinear in the voltages. The DC power flow equation provide a linearized approximation of the active power flows in the AC model. Linearization is possible under the following conditions [12]:

1. The difference between the voltage phase angles of every couple of neighboring nodes is small, such that $\sin\theta_{ik} \approx \theta_{ik}$ and $\cos\theta_{ik} \approx 1$.

2. The active power losses are negligible and, therefore, $\mathbf{Y} \approx \mathbf{iB}$, where $\mathbf{B}$ is the imaginary part of the admittance matrix $\mathbf{Y}$ as calculated when neglecting the line resistances.

3. The variations in the voltage magnitudes $|V_i|$ are small and, therefore, it is assumed that $|V_i| = 1 \; \forall i$.

Under these assumptions, given the active power P_i at each node i, the phase angles of the nodes can be estimated by $\tilde{\theta}_i$ using the DC power flow equations as follows:

$$P_i = \sum_{\substack{k=1 \\ k \neq i}}^{n} P_{ik}^{(\mathrm{DC})} = \sum_{\substack{k=1 \\ k \neq i}}^{n} B_{ik}(\tilde{\theta}_i - \tilde{\theta}_k) \qquad (4)$$

or in matrix form,

$$\tilde{\mathbf{P}} = -\mathbf{B}\tilde{\mathbf{\Theta}} \qquad (5)$$

where $\tilde{\mathbf{P}} = [\tilde{P}_1, P_2, \ldots, P_n]^{\mathrm{T}}$, $\tilde{\mathbf{\Theta}} = [\tilde{\theta}_1, \ldots, \tilde{\theta}_n]^{\mathrm{T}}$.

3. MODELING CASCADING FAILURES

An initial failure in a power grid may result in subsequent failures in other parts of the grid. These consecutive failures following an initial failure constitute a *cascading failure*. In this section, we follow [7, 8, 11, 14] and develop models for cascading failures due to line failures in power grids.

Before a cascading failure, we assume that $\mathcal{G}(\mathcal{N}, \mathcal{L})$ is connected, the power flows satisfy (2) and (3) or (5), and the flow magnitude $|f_l|$ of each line is at most its capacity c_l.

Next, we describe the cascading failures models. When an initial set of lines fail, they are removed from the network. As a result of this removal, the network topology is changed and the power grid can be divided into one or more connected components. Following [14], we assume that each connected component can operate autonomously. If there is no supply or no demand within a connected component $\mathcal{G}_k$, the component becomes a *dead component* and all the demand or supply nodes within the component are (put) out of service. If there are both supply and demand nodes within a connected component $\mathcal{G}_k$, the connected component remains an *alive component*, but the supply and demand within the component should be balanced. We use two different supply and demand balancing rules [8, 14]:

1. *Shedding and curtailing:* The amount of power supply/demand is reduced at all nodes by a common factor. If the total active power supply is more than the total active power demand in a connected component $\mathcal{G}_k$, the active power outputs of generators are curtailed. On the other hand, if the total active power supply is not sufficient to serve the total active power demand, load shedding is performed to balance the supply and demand within $\mathcal{G}_k$.

2. *Separating and adjusting:* Excess supply or demand nodes are separated from the grid. In this case, we assume that the dynamic responses of the generators (demand nodes) are related to their sizes [13]. Namely, the generators (demand nodes) with lower amounts of power output are assumed to be faster to respond to the imbalances between supply and demand. Thus, within each component $\mathcal{G}_k$ with excess supply (demand), the generators (demand nodes) are separated from the grid according to their sizes from smallest to largest until the removal of one more generator (demand node) results in the shortage of supply (demand). Then, the active power output (demand) of the largest supply (demand) node is reduced in order to balance supply and demand.

After supply and demand are balanced within each alive component, using the selected balancing rule, the power flow equations are solved to compute new flows on the lines. Note that the line capacities are not taken into account in determining the flows. The new set of line failures are then found in all alive components. We use two different line outage rules [8, 11]:

1. *Deterministic:* A line l fails when the power flow magnitude on that line, denoted by $|f_l|$, exceeds its capacity c_l.

2. *Probabilistic:* A line l fails with probability p_l at each stage of the cascade. We assume that each line l with a flow capacity c_l has also a nominal power flow level $\xi_l \in [0, c_l]$, after which the line may fail with a certain probability (due to the increase in line temperature or sag levels). Under this model, the probability p_l is approximated as:

$$p_l = \begin{cases} 0, & \text{if } |f_l| < \xi_l \\ \frac{|f_l| - \xi_l}{c_l - \xi_l}, & \text{if } \xi_l \le |f_l| < c_l \\ 1, & \text{if } |f_l| \ge c_l. \end{cases} \quad (6)$$

After finding the new set of line failures using the selected line outage rule, the cascade continues with the removal of those lines. If there are no new line failures in any of the alive components, the cascade ends.

In this paper, we study three cascade processes:

I) Cascade with the shedding and curtailing balancing rule and the deterministic line outage rule,

II) Cascade with the separating and adjusting balancing rule and the deterministic line outage rule,

III) Cascade with the shedding and curtailing balancing rule and the probabilistic line outage rule.

In order to study the differences between the AC and DC models, we mostly focus on the cascade process I. In order to further capture the effects of the cascade processes on the differences obtained under the AC and DC models, in Subsection 4.3, we briefly compare the three cascade processes.

In the following two subsections, we provide the details of the cascade models under the AC and DC power flows.

3.1 AC Cascading Failures Model

In the cascade under the AC power flow model, the flows are composed of active parts P_i in (2) and reactive parts Q_i in (3). Hence, the apparent power S_i in (1) is used to calculate the flows. In general, due to transmission line impedances, the voltage at the sending node of a line is different than the one at the receiving node, resulting in different values of the apparent power flows at each side of the line. Hence, in the cascade under the AC model, we define the magnitude $|f_l|$ of the flow on a line $l = \{i, k\}$ as follows:

$$|f_l| = \frac{|S_{ik}| + |S_{ki}|}{2}. \quad (7)$$

The difference, $S_{ik} - S_{ki}$, between the sent and received apparent flows on a line l represents the power loss over that line. The sum of the losses over all the lines is the total loss in the network. The total loss cannot be calculated in advance and is only known after the power flow equations in (1) are solved. Therefore, in the cascade under the AC model, a part of the total supply in the network is reserved to supply the network losses and denoted by the *reserved loss factor* η.

The case of zero reserved loss factor, $\eta = 0$, means that no reserve supply is allocated for network losses, whereas a large reserved loss factor η corresponds to a large reserve supply

for the network losses. Once the power flow equations are solved and the network losses are calculated, the difference between the allocated supply and the total demand with losses is compensated by the slack-node. Therefore, in the AC cascading failures model, the simulation is slack-node dependent and, for every alive component without such a node, a slack-node must be assigned. The developed model chooses the slack-node as the voltage-controlled node with the maximum power output in that alive component.

The iterative process of solving the AC power flow equations (2) and (3) may result in the absence of a solution or a divergence in iterations. In such cases, it is perceived that the connected component cannot function at those operational conditions and supply and demand shedding is applied. The amount of active and reactive power demands and active power supply within that component are decreased until either convergence is reached in the power flow equations or the component becomes a dead component with no demand.

3.2 DC Cascading Failures Model

In the cascade under the DC power flow model, the magnitude $|f_l|$ of the flow on a line $l = \{i, k\}$ is equal to the magnitude of the active power flow in (4) on that line:

$$|f_l| = |P_{ik}| = |P_{ki}|. \quad (8)$$

Since the network is assumed to be lossless, the magnitude of the active power at the sending side of a line is equal to the magnitude of the active power at the receiving side, $|P_{ik}| = |P_{ki}|$, and the total supply is equal to the total demand. Therefore, supply and demand balancing is performed without a reserved loss factor η. Moreover, the lossless assumption means that the power flows in the network are slack-node independent.

Contrary to the AC power flow equations (2) and (3), which are nonlinear, the DC power flow equations (5) are linear, and a solution always exists for a connected network with balanced supply and demand [9]. Hence, no supply or demand shedding due to convergence issues is needed in the DC model.

4. NUMERICAL COMPARISON OF THE AC AND DC POWER FLOW MODELS

This section presents a numerical comparison of the AC and DC power flow models. We first provide the simulation setup. Then, we compare the evolution of the cascade process I initiated by single line failures under the AC and DC power flow models. Next, we compare the three cascade processes under the AC and DC flow models.

4.1 Simulations Setup

4.1.1 Metrics

We define metrics for evaluating the grid vulnerability (some of which were originally used in [7, 9, 17, 19]). To study the *cascade severity*, we define:

▶ **Node-loss ratio** ($N_{\mathcal{G}}$): the ratio of the total number of failed nodes (i.e., nodes in dead components) at the end of the cascade to the total number of nodes.

▶ **Line-loss ratio** ($L_{\mathcal{G}}$): the ratio of the total number of failed lines at the end of the cascade to the total number of lines.

▶ **Yield** ($Y_{\mathcal{G}}$): the ratio of the demand supplied at the end of the cascade to the initial demand.

In addition to the previous metrics, which capture the overall effect of a cascading failure on a power grid, we identify the frequently overloaded lines that may cause cascading failures to persist. Hence, we define

▶ **Line-vulnerability ratio** (R_l): the total number of cascading failures in which line l is overloaded over the total number of cascading failures simulations. Higher values of R_l indicate the vulnerability of the line l as a possible bottleneck in the network.

4.1.2 Properties of the Networks used in Simulations

We considered four realistic networks: the IEEE 30-bus, the IEEE 118-bus, and the IEEE 300-bus test systems [1], as well as the Polish transmission grid [20]. The details of these networks are as follows.

▶ **The IEEE 30-bus test system** contains 30 nodes and 41 lines with a total power demand of 189.2 MW.

▶ **The IEEE 118-bus test system** contains 118 nodes and 186 lines with a total power demand of 4242 MW.

▶ **The IEEE 300-bus test system** contains 300 nodes and 411 lines with a total power demand of 23,525.85 MW.

▶ **The Polish transmission grid**, at summer 2008 morning peak, contains 3120 nodes and 3693 lines with a total power demand of 21,181.5 MW.

In the IEEE test networks, maximum line flow capacities are not present. Following [14], the line flow capacities are estimated as $c_l = (1 + \alpha) \max\{|f_l|, \overline{f}\}$, where $\alpha = 1$ is the line tolerance, and $\overline{f}$ is the mean of the initial magnitude of line flows.

In the Polish transmission grid data, emergency ratings are used for the flow capacities of the network. In order to eliminate existing overloaded transmission lines at the base case operation, the line flow capacities of such overloaded lines are changed to $c_l = (1 + \alpha)|f_l|$, where $\alpha = 1$.

4.1.3 Power Flow Solver

To conduct our simulations, we have used MATPOWER [20] package in MATLAB for solving the AC and DC power flows.
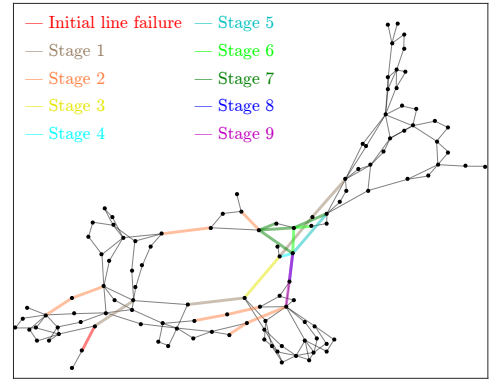
4.2 Cascading Failures Initiated by Single Line Failures

An example of a cascade initiated by a single line failure in the IEEE 118-bus network under the two cascade models is shown in Fig. 1. The basic observation from this figure is that the evolution of the cascade under the two models can be quite different. For instance, in Fig. 1a, there are two overloaded lines at the first stage of the cascade under the AC model which are not overloaded under the DC model. This initial difference results in a considerable difference in the evolution of the cascade: An important flow path in the AC model fails at the first stage, resulting in more severe consecutive failures. Therefore, the differences between the AC and DC models accumulate at each cascade stage and may lead to *a significantly different result at the end of the cascade.*

To further investigate the differences, we simulate cascading failures due to all single line failures whose initial flows were larger than the mean of initial flows in the four test networks. Figs. 2-4 provide the detailed results obtained under the two cascade models.
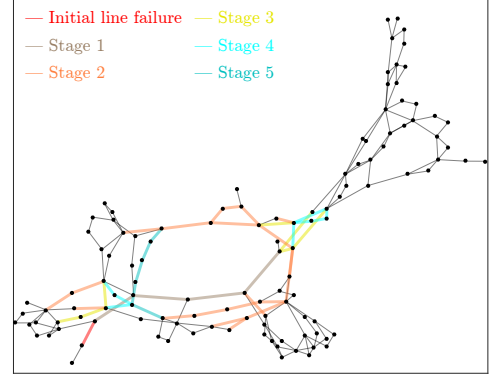
(a) AC cascading failures model

(b) DC cascading failures model

Figure 1: Evolution of a cascade initiated by a single line failure in the IEEE 118-bus network under the AC and DC cascade models. The remaining load at the end of the simulation is 1594.5 MW under the AC cascading failures model, and 2446.3 MW under the DC cascading failures model.

Fig. 2 shows the scatter plot of the yield values under the two models for the IEEE 118-bus network and the Polish grid. It suggests that the yield values obtained by the DC cascade model are usually higher, especially for large networks. Moreover, Fig. 4a, which presents the CDFs of the differences in yield values for all the test networks, also shows that the differences in the obtained yield values can become quite big in large networks.

However, in Fig. 4b, which presents the CDFs of the differences in line-loss ratios for all the test networks, the line-loss ratios are observed to be close under the two cascade models in all the four networks. The same is true for the node-loss ratios (see Fig. 4c). Despite the similarity of the line-loss and node-loss ratios under the two cascade models, Fig. 3, which presents the line-vulnerability ratios in the IEEE 118-bus network and the Polish grid, suggests that as networks become larger, the individual lines that fail frequently under the AC model are very different from their counterparts under the DC model (see Fig. 3b). Fig. 4d also shows that
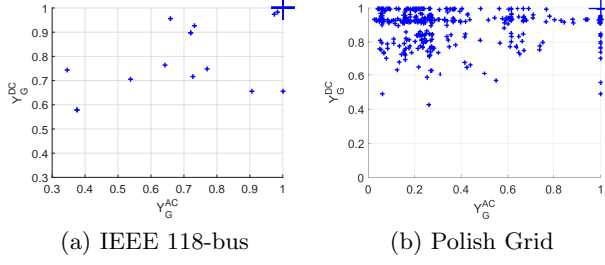
(a) IEEE 118-bus (b) Polish Grid

Figure 2: The scatter plots of the yield values under the AC versus DC cascade models initiated by single line failures. Markers are scaled according to the frequencies of corresponding data points.
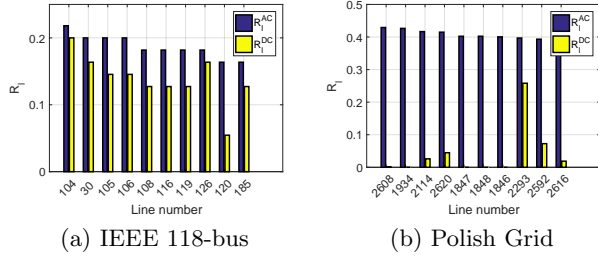

(a) IEEE 118-bus (b) Polish Grid

Figure 3: Comparison between the line-vulnerability ratios under the AC and DC cascade models initiated by single line failures. The lines with the highest line-vulnerability ratios under the AC cascade model are selected for comparison.

the differences in the line-vulnerability ratios are close for most of the lines, but the differences may be quite big for roughly 10% of the lines in large networks.

4.3 Comparison Between the Three Cascade Processes under the AC and DC Models

In this subsection, we compare the three cascade processes defined in Section 3, initiated by single line failures under the AC and DC models. For cascade process III, we set the threshold ξ_l of a line l in (6) as $\xi_l = 0.8 \times c_l$.

Figs. 5-6 provide detailed comparisons between the results obtained under the AC and DC cascade models for the three cascade processes. Fig. 5a shows the scatter plot of the yield values for cascades in the IEEE 118-bus network. The yield values obtained by cascade process II are generally lower than the other two cascade processes under the AC model. Fig. 5b, which presents the CDF of the differences in yield values under the AC and DC cascade models for the three cascade processes in the IEEE 118-bus network, also shows that the differences in the obtained yield values under the AC and DC models can become big for cascade process II.

Figs. 6a and 6b present the CDFs of the differences in line-loss and line-vulnerability ratios in the IEEE 118-bus network, respectively. Similar to Fig. 5b, the magnitudes of the differences in the obtained line-loss ratios under the AC and DC models are highest for cascade process II. The difference between the individual line-vulnerability ratios in Fig. 6b can grow arbitrarily high for cascade process III.

Figs. 5-6 suggest that different rules for the supply and

(a) $X := |Y_{\mathcal{G}}^{\text{AC}} - Y_{\mathcal{G}}^{\text{DC}}|$ (b) $X := |L_{\mathcal{G}}^{\text{AC}} - L_{\mathcal{G}}^{\text{DC}}|$

(c) $X := |N_{\mathcal{G}}^{\text{AC}} - N_{\mathcal{G}}^{\text{DC}}|$ (d) $X := |R_l^{\text{AC}} - R_l^{\text{DC}}|$
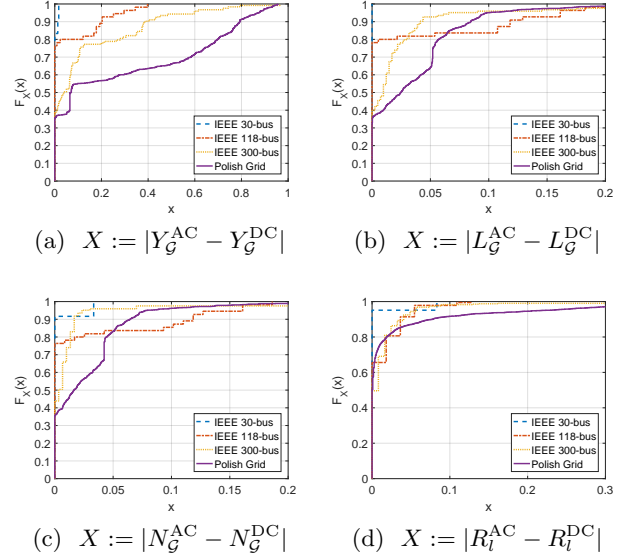
Figure 4: The CDFs of the differences between the metrics after cascading failures initiated by single line failures under the AC and DC models for all the test networks.

demand balancing and line outages could have different effects on the evaluation of the cascades under the AC and DC models. In particular, cascade process II increases the differences between the AC and DC models most. In that cascade process, by disconnecting many small-sized generators distributed in the network, the demands are supplied by few large-sized generators during the cascade stages. Consequently, the remaining network suffers from low voltage magnitudes and overloaded lines, which can lead to divergence in iterations of AC power flow equations. Moreover, the reactive power flows and voltage magnitudes are not modeled by the DC power flow model, which can lead to larger differences between the cascades under the AC and DC power flow models. Although cascade process III does not affect the yield values and line-loss ratios, its effect is more significant in identifying the most vulnerable set of lines. Due to the probabilistic line tripping model in (6), different lines may trip at each cascade stage, which can result in detecting different sets of vulnerable lines under the AC and DC models.

5. CONCLUSION

In this paper, we have studied cascading failures in power grids under nonlinear (AC) and linearized (DC) power flow models. Our cascading failures simulations demonstrate that even slight errors in individual line flows under the AC and DC models can accumulate during the cascade stages and result in significant differences at the end of the cascade. Moreover, the metrics that capture the operational and topological aspects of the cascade can differ significantly under the two models.

Overall, the obtained results suggest that due to the voltage constraints, the divergence problems, and the reactive power flows, the cascades under the AC power flow model are more severe compared to the ones under the DC power flow model. Hence, the DC model may underestimate the

(a) $Y_{\mathcal{G}}^{\mathrm{AC}}$ vs $Y_{\mathcal{G}}^{\mathrm{DC}}$ (b) $X := |Y_{\mathcal{G}}^{\mathrm{AC}} - Y_{\mathcal{G}}^{\mathrm{DC}}|$
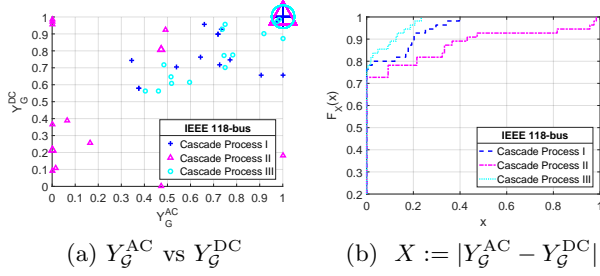
Figure 5: The (a) scatter plots of the yield values and (b) CDFs of the differences between the yield values under the AC and DC cascade models for the three cascade processes initiated by single line failures in the IEEE 118-bus network. Markers are scaled according to the frequencies of corresponding data points.

(a) $X := |L_{\mathcal{G}}^{\mathrm{AC}} - L_{\mathcal{G}}^{\mathrm{DC}}|$ (b) $X := |R_l^{\mathrm{AC}} - R_l^{\mathrm{DC}}|$
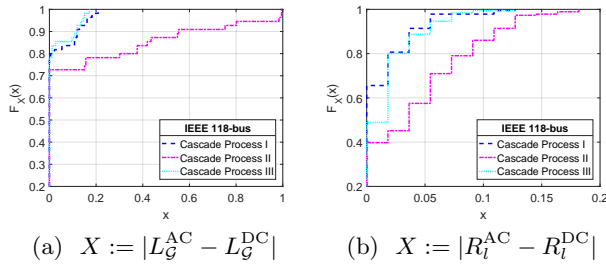
Figure 6: The CDFs of the differences between the metrics after cascades under the AC and DC models for the three cascade processes initiated by single line failures in the IEEE 118-bus network and Polish grid.

severity of the cascade, especially for larger networks. Thus, special care should be taken when drawing conclusions based on the DC cascade model in power grids.

Acknowledgement

6. REFERENCES

[1] Power systems test case archive. Available at: http://www.ee.washington.edu/research/pstca/.
[2] Report on blackout in Turkey on 31st March 2015. Technical report, ENTSO-E, 2015.
[3] Final report on the August 14th blackout in the United States and Canada: Causes and recommendations. Technical report, U.S.- Canada Power System Outage Task Force, April 2004.
[4] F. Alvarado and S. Oren. Transmission system operation and interconnection. *National transmission grid study–Issue papers*, pages A1–A35, 2002.
[5] A. Bakshi, A. Velayutham, S. Srivastava, K. Agrawal, R. Nayak, S. Soonee, and B. Singh. Report of the enquiry committee on grid disturbance in Northern Region on 30th july 2012 and in Northern, Eastern & North-Eastern Region on 31st July 2012. *New Delhi, India*, 2012.
[6] R. Baldick, B. Chowdhury, I. Dobson, Z. Dong, B. Gou, D. Hawkins, H. Huang, M. Joung, D. Kirschen, F. Li, et al. Initial review of methods for cascading failure analysis in electric power transmission systems IEEE PES CAMS task force on understanding, prediction, mitigation and restoration of cascading failures. In *Proc. IEEE PES-GM'08*, July 2008.
[7] A. Bernstein, D. Bienstock, D. Hay, M. Uzunoglu, and G. Zussman. Power grid vulnerability to geographically correlated failures - analysis and control implications. In *Proc. IEEE INFOCOM'14*, Apr. 2014.
[8] D. Bienstock. *Electrical Transmission System Cascades and Vulnerability: An Operations Research Viewpoint*, volume 22. SIAM, 2016.
[9] H. Cetinay, F. A. Kuipers, and P. Van Mieghem. A topological investigation of power flow. *to appear in IEEE Systems Journal*, 2017.
[10] P. Crucitti, V. Latora, and M. Marchiori. A topological analysis of the Italian electric power grid. *Physica A: Statistical Mechanics and its Applications*, 338(1):92–97, 2004.
[11] I. Dobson. *Encyclopedia of Systems and Control*. Cascading network failure in power grid blackouts. Springer, 2015.
[12] J. D. Glover, M. S. Sarma, and T. Overbye. *Power System Analysis & Design, SI Version*. Cengage Learning, 2012.
[13] J. J. Grainger and W. D. Stevenson. *Power system analysis*. McGraw-Hill, 1994.
[14] Y. Koç, T. Verma, N. A. Araujo, and M. Warnier. Matcasc: A tool to analyse cascading line outages in power grids. In *Proc. IEEE IWIES'13*, 2013.
[15] K. Purchala, L. Meeus, D. Van Dommelen, and R. Belmans. Usefulness of DC power flow for active power flow analysis. In *IEEE PES-GM'05*, June 2005.
[16] S. Soltan, A. Loh, and G. Zussman. Analyzing and quantifying the effect of k-line failures in power grids. *to appear in IEEE Trans. Control Netw. Syst.*, 2017.
[17] S. Soltan, D. Mazauric, and G. Zussman. Analysis of failures in power grids. *in IEEE Trans. Control Netw. Syst.*, 4(3):288–300, 2017.
[18] D. Van Hertem, J. Verboomen, K. Purchala, R. Belmans, and W. Kling. Usefulness of DC power flow for active power flow analysis with flow controlling devices. In *Proc. IET ACDC'06*, pages 58–62, 2006.
[19] A. J. Wood and B. F. Wollenberg. *Power generation, operation, and control*. John Wiley & Sons, 3rd edition, 2012.
[20] R. D. Zimmerman, C. E. Murillo-Sánchez, and R. J. Thomas. Matpower: Steady-state operations, planning, and analysis tools for power systems research and education. *IEEE Trans. Power Syst.*, 26(1):12–19, 2011.